frontiers | Frontiers in Marine Science

TYPE Original Research
PUBLISHED 10 October 2022
DOI 10.3389/fmars.2022.1033164

OPEN ACCESS

EDITED BY
Guangzhe Jin,
Guangdong Ocean University, China

REVIEWED BY
Zuhao Zhu,
Ministry of Natural Resources, China
Zhipeng Cheng,
Nankai University, China

*CORRESPONDENCE
Wen Zhuang
wzhuang@sdu.edu.cn

SPECIALTY SECTION
This article was submitted to Marine Pollution, a section of the journal Frontiers in Marine Science

RECEIVED 31 August 2022
ACCEPTED 26 September 2022
PUBLISHED 10 October 2022

CITATION
Liu M, Song X, Wang Q, Li S, Kou S, Gao Z and Zhuang W (2022) Sorption behavior and mechanisms of thallium to microplastics.
Front. Mar. Sci. 9:1033164.
doi: 10.3389/fmars.2022.1033164

Sorption behavior and mechanisms of thallium to microplastics

Min Liu[1,2,3], Xiaocheng Song[1,2,3], Qian Wang[4], Shilei Li[5], Siwang Kou[5], Zhenhui Gao[1,2] and Wen Zhuang[1,2,3]*

[1]Institute of Eco-environmental Forensics, Shandong University, Qingdao, China, [2]School of Environmental Science and Engineering, Shandong University, Qingdao, China, [3]Pilot National Laboratory for Marine Science and Technology, Qingdao, China, [4]Qingdao Research Institute of Wuhan University of Technology, Qingdao, China, [5]Ecological Environment Damage Judicial Appraisal Center, Hebei Zhong Xu inspection testing technologies Co, Ltd., Shijiazhuang, China

Thallium (Tl) is a metal of high toxicity, and the problem of Tl pollution is being faced globally. However, environmental data on Tl are still scarce and its biogeochemical behaviors remain mostly unclear. Studies have revealed the potential transport of other heavy metal by microplastics (MPs), but there is no report on the interactions between Tl and MPs yet. Therefore, we studied the adsorption of Tl by the three most commonly detected MPs, i.e., polyethylene (PE), polystyrene (PS), and polypropylene (PP) in fresh and seawater. We considered the effects of particle size, pH and competitive cations on adsorption capacity. The results showed PS has the highest adsorption capacity for Tl which was mainly through surface complexation. PS showed the lowest crystallinity and had the most oxygen-containing functional groups among the studied MPs. The adsorption of Tl on PE and PP was dominated by physical adsorption. The adsorptions exhibited significant salinity and pH dependence. Dominant cations in seawater competed with Tl ions for adsorption sites on MPs. With the increase in pH, the deprotonation of the carboxyl functional groups on MPs was enhanced, which increased the effective adsorption sites and promoted the adsorption of Tl. However, the adsorption capacity of the studied MPs for Tl was much lower than the corresponding capacity of natural minerals (clay, iron and manganese oxides) previously reported. Therefore, MPs may not be the main factors affecting the environmental behavior of Tl. This study provides valuable information for the study of thallium's environmental behavior and ecological risk assessment.

KEYWORDS

thallium, microplastics, adsorption kinetics, adsorption isotherm, fresh water, seawater

Introduction

Thallium (Tl) is a trace metal element widely distributed in natural environments. The average abundance of Tl in the continental crust is ~0.49 mg/kg, in soil and offshore sediment are 0.22-0.55 mg/kg, and the concentration in unpolluted water is not higher than 20 ng/L (Peter and Viraraghavan, 2005; Belzile and Chen, 2017). Although with low environmental abundance, Tl is a very toxic heavy metal. Tl has two valence states, monovalent and trivalent. In the biotoxicity experiment of unicellular algae (Chlorella sp.) in freshwater environment, Tl (I) and Tl(III) showed no significant difference in the inhibition rate of the growth rate of Chlorella ($p=0.05$) between the 2×10^{-13} mol/L Tl^{3+} solution and 1×10^{-8} mol/L Tl^{+} solution, indicating that Tl(III) was much more toxic than Tl(I). Under the same experimental conditions, the inhibition rate of 8.7×10^{-9} mol/L Cd^{2+} solution was comparable to the toxicity of Tl mentioned above (Ralph and Twiss, 2002). Thus, considering the concentration, the order of toxicity was as follows: Tl(III) > Cd(II) > Tl(I). Which was also the same as the results of the large flea toxicity test (Borgmann et al., 1998). Tl(I) is thermodynamically more stable than Tl (III), so Tl(I) is much more abundant than Tl (III) in nature (Lan and Lin, 2005). Because Tl^{+} ions and K^{+} ions have similar ion radii and high affinity for sulfur ligands, they are easy to be absorbed, transmitted and accumulated by the organisms (Peter and Viraraghavan, 2005; Liu et al., 2021; Yang et al., 2022; Yao et al., 2022).

Thallium has both lithophilic and sulphurophilic properties and is widely present in silicate and sulfide minerals (Liu et al., 2018; Yao et al., 2022). Tl is often enriched in sulfide deposits as an associated mineral of lead, zinc, copper and other metals (Li et al., 2019). In general, only the presence of sulfide melts is the main host for Tl (Kiseeva and Wood, 2013). Compared with other sulfide minerals, the content of Tl in pyrite is relatively high. The enrichment of thallium in pyrite may be due to a number of factors, including low-temperature epithermal metallic origin (Liu et al., 2016). The main sources of Tl produced by human activities include the smelting of Tl-containing ores, slag weathering and leaching, discharge of industrial wastewater, and coal combustion (Song et al., 2022). Tl pollution incidents caused by mining, ore smelting or corporate sewage have occurred all over the world (Liu et al., 2017; Ghezzi et al., 2019; D'Orazio et al., 2020; Horn et al., 2020; Wang et al., 2020). In Tl polluted areas, the concentration of Tl can be as high as hundreds of ppm (Liu et al., 2019). In the past, Tl was used for the production of pesticides. In recent years, approximately 70% of Tl production is used in electronic devices (Willner et al., 2021).

After entering the environment, Tl interacts with other substances, thereby affecting the biogeochemical behavior of Tl. The adsorption mechanisms of Tl by common minerals (e.g., clay minerals, iron oxides, manganese oxides, etc.) in soils and natural waters have been mostly reported (Zhuang et al., 2021). Manganese oxides are the strongest natural mineral oxidants in the environments (Peacock and Moon, 2012; Wu et al., 2019; Yan et al., 2021). Many studies on soils and sediments have found very high correlations between Tl and Mn in the reducible mineral fraction (Cruz-Hernández et al., 2019). Tl(I) can be oxidized to Tl (III) by hexagonal birnessite to form Tl_2O_3, followed by the formation of Tl-rich amorphous manganese oxide (Wick et al., 2019). Iron (hydrated) oxides such as goethite and iron hydride have strong Tl adsorption capacity. Tl in sediments tends to correlate significantly with Fe content because Tl can be adsorbed to iron mineral surfaces through surface complexation (Lin et al., 2020). Because the radius of Tl^{+} ion and K^{+} ion is similar, the affinity of Tl^{+} is between Cs^{+} and Rb^{+}, so Tl can also strongly bind to illite (Wick et al., 2018).

Microplastics (MPs) pollution, which is exacerbated by massive plastic production and improper disposal, has now become a globally recognized new type of environmental problem (Cao et al., 2021; Wang et al., 2021; Song et al., 2022). MPs have the characteristics of large specific surface area, high porosity, amorphous structure which hydrophobic surface, so they can adsorb a series of pollutants (such as heavy metals, organic matter and antibiotic resistance genes) with different physicochemical properties and affect the behavior of these pollutants (Liu et al., 2020; Cao et al., 2021; Kutralam-Muniasamy et al., 2021; Liu et al., 2021). The combined toxicity of the co-pollutants is often higher than that of a single pollutant (Song et al., 2022). Ag nanoparticles can hetero-aggregate with PS through electrostatic interactions with O–containing groups (C–O, C–OH and C=O), thus co-precipitate from water phase (Zhang et al., 2021). The interaction between Pb/Cu and PE was physisorption, and they can attach through weak bonds and easy to release into the aquatic ecosystem (Purwiyanto et al., 2020). The interactions between MPs and heavy metals are affected by characteristics of the MPs (particle size, specific surface area, functional groups, aging, concentrations, additives) and external factors (pH, salinity, temperature and redox status (Gao et al., 2021; Li et al., 2022; Liu et al., 2022; Song et al., 2022).

At present, there is no research on the role of MPs as carriers of Tl in the environments, and the adsorption capacity of MPs for Tl is still not clear, which limits the cognition on the environmental behavior of Tl. The types of plastics affect their- abundances in the environment, PP is usually found in high concentrations in water bodies, while PE is relatively high in sediments. Both PP and PE are the most commonly detected MPs in the environments (Nkwachukwu et al., 2013; Koutnik et al., 2021; Xi B. et al., 2022; Xi X. et al., 2022). Moreover, in the current marine ecosystem, PS also has become one of the most common MPs pollutants (Wagner et al., 2014). The purpose of this paper is to study the adsorption mechanism of Tl by three most commonly detected MPs in the environment, i.e., polyethylene (PE), polystyrene (PS), and polypropylene (PP).

The influence of particle size of MPs, the pH and salinity of water (competitive ions) on the adsorption effect was further studied. The results of this research can help to improve the understanding of the mechanism of Tl's migration and transformation in aquatic environments, and also provide theoretical support for the ecological risk assessment and pollution control of Tl.

Materials and methods

Materials preparation and characterization

Three species of MPs were used in the present study, i.e., PE, PS and PP. They were obtained from Zhonglian plasticization Co., Ltd (China). The mean particle sizes of PE, PS are 25 μm, 150 μm and 550 μm, and the mean particle sizes of PP are 13 μm, 150 μm and 550 μm. Thallium nitrate ($TlNO_3$) standard solution was purchased from Sinopharm Chemical Reagent Co., Ltd (China). All other chemical reagents were of analytical or higher grade when available. Seawater was collected from Aoshan Bay, the Yellow Sea in China, and was filtered through 0.22 μm polycarbonate filter membranes (Whatman, diameter 47 mm).

MPs were put into 250 ml glass beakers, a certain amount of ethanol (75%) was added with magnetic stirring at 200 rpm/min for 48 h, then 1% HNO_3 solution was added for another 24 h. Finally, Milli-Q water (18.2MΩ cm^{-1}) was used to wash the MPs several times. Shape and surface morphology of MPs were observed by Scanning Electron Microscopy (SEM, FEI Quanta 250FEG). Additionally, attenuated total reflectance-Fourier transform infrared spectra (ATR-FTIR) was used to analyze the functional groups on the surface of MPs. The resolution is 4 cm^{-1} and the scan range is from 600 to 4,000 cm^{-1} (Chen et al., 2021). Data were analysed with OMIC software.

Batch experiment

Adsorption kinetics (25 ± 2°C). PE (25 μm, 550 μm), PS (25 μm, 550 μm) and PP (13 μm, 550 μm) were used in adsorption kinetics experiment. The concentrations of the $TlNO_3$ used were 1.0 mg/L (namely low initial Tl(I)) and 20 mg/L (namely high initial Tl(I)), respectively, and the pH was adjust to ~8.00 ± 0.10 with 1 mol/L NaOH or HNO_3. Add ~0.050 ± 0.0005 g MPs to 250 ml $TlNO_3$ solution and react for 48 h (magnetic stirring at 200 rpm/min). At the time points of 0.5, 1.0, 2.0, 3.0, 4.0, 6.0, 8.0, 10, 12, 24, 36 and 48 h, the reaction solutions were kept still for 5 min, and then 2.5 mL supernatants were filtered through 0.22 μm polyethersulfone filters to remove MPs in the experiment. The filtered supernatants were brought to a volume of 15 mL with 1% HNO_3 (v/v). Three parallel samples (n = 3) were set for all experiments.

Adsorption isotherm (25 ± 2°C). Experiments were performed in sets of triplicates for 7 days:

1. Particle size group. PE (25 μm, 150 μm and 550 μm), PS (25 μm, 150 μm and 550 μm) and PP (13 μm, 150 μm and 550 μm). The pH was adjusted to 8.00 ± 0.10.
2. pH group. PE (150 μm), PS (150 μm) and PP (150 μm). Three different pH values were set for each particle size, namely 4.00 ± 0.10, 6.00 ± 0.10 and 8.00 ± 0.10.
3. Seawater group. One set was the original collected and filtered seawater with the salinity of 32‰. The other set was seawater with the salinity of 15‰ after dilution with Milli-Q water. The MPs used were PE (150 μm), PS (150 μm) and PP (150 μm), and the pH was adjusted to 8.00 ± 0.10. The final concentration of microplastics in all reactions was ~0.2 g/L. Tl(I) concentrations were 0, 0.05, 0.1, 0.2, 0.5, 1.0, 2.0, 5.0, 10, 20, and 50 mg/L. After the end of each experiment, the final pH values were measured. More details are provided in the Supporting Material.

Three kinetic models were used to fit the sorption kinetics data, namely, Pseudo-first-order kinetic model (PFO), Pseudo-second-order kinetic model (PSO) and The Weber and Morris model (TWM) (Weber and Boell, 1962; Bhagwat et al., 2021; Tang et al., 2021b). The adsorption isotherms were fitted using Freundlich and Langmuir models (Dong et al., 2020; Purwiyanto et al., 2020; Yu et al., 2021). Details of the models are given in Table S2. The surface concentrations of C, O, Tl were measured by X-ray photoelectron spectroscopy (XPS, E Thermo Fisher ESCALAB XI+), and the experimental peaks were fitted with the Avantage software. An inductively coupled plasma mass spectrometer (ICP-MS, Agilent Technologies-G8421A 7800) was used to determine the concentrations of Tl, K, Na, Ca, Mg, Sr. Origin software (2021 version) was used for mapping and data processing.

Results and discussion

Adsorption kinetics

Kinetic studies were conducted in order to evaluate the adsorption rate and mechanism between MPs (PE, PS and PP) and Tl. The adsorption kinetics were fitted using PFO, PSO and TWM kinetic model as previously described. The parameters of each model are summarized in Table S4.

Different types and particle sizes of MPs and different initial Tl concentrations led to large differences in the final

quasi-equilibrium time (Figure 1). With the low initial Tl concentration (1.0 mg/L), the adsorption between PS (550 μm) and Tl(I) reached quasi-equilibrium after 24 h, while the adsorption between PS (25 μm) and Tl(I) used 10 h. The time to reach quasi equilibrium was nearly 12 h for PS (25 μm) group and PE (550 μm). With the high initial Tl concentration (20 mg/L), The time to reach quasi equilibrium for PS (25 μm) group was 24 h, and for PS (550 μm) group was 12 h. The time to reach quasi equilibrium for PE (25 μm) group and PE (550 μm) were basically 12 h. At the low initial Tl(I) concentration, the smaller the particle size of PS, the shorter the equilibration time required to reach equilibrium, indicating that MPs with small crystal and particle size improved kinetics of Tl(I) sorption. The time required for the two particle sizes of PE to reach quasi-equilibrium was the same, indicating that particle size was not a key factor in controlling the rate of adsorption between PE and Tl(I). At high initial Tl(I) concentration, the equilibrium time for PS (25 μm) group was longer than that of PE (550 μm) group. One probable reason was that the aggregation of PS led to the reduction of the number of adsorption sites, and the smaller the particle size, the more obvious the aggregation phenomenon was (Huang et al., 2021; Kim et al., 2022). The morphology of PP is smooth and fibrous, the functional groups on the surface are mainly -CH2, whereas the highly active functional groups (-C=O-, -C-O-, -OH and -COOH, etc.) are few, thus adsorption capacity is poor. In addition, the density of PP is lower than that of water. During the experiment, PP floated above the solution and had less contact with Tl (I) ions in the solution, resulting in poor adsorption effect. The final experimental results did not conform to the three kinetic models selected. Therefore, only the maximum adsorption capacity of Tl(I) by PP is shown in Figure 1. In PP (13 μm) and PP (550 μm) group, the maximum adsorption capacity was mainly controlled by the initial concentration of Tl(I) and the particle size of PP.

The adsorption kinetic data of PE and Tl(I) were better fitted by PFO model (show in Table S4), PFO model indicates that the reaction rate was linearly related to the concentration of reactants, and it was speculated that the adsorption of Tl(I) by PE was mainly a physisorption process (Bhagwat et al., 2021). Physical adsorption mainly relies on electrostatic action and van

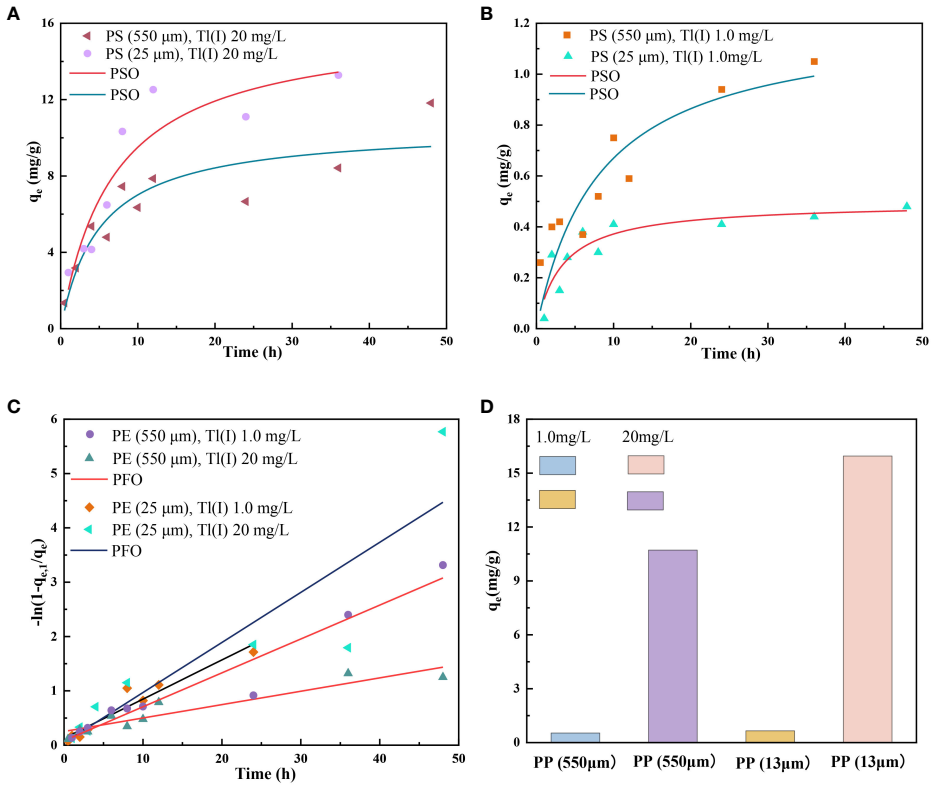

FIGURE 1
Adsorption kinetics. **(A)** PS + low initial Tl(I); **(B)** PS + high initial Tl(I); **(C)** PE + low and high initial Tl(I); **(D)** PP + low and high initial Tl(I). PFO means Pseudo-first-order kinetic model; PSO means Pseudo-second-order kinetic model. Adsorption results of Tl by PP did not fit into any of the kinetic models.

der Waals force to adsorb heavy metal ions. The PE adsorbed Tl^+ in solution to the surface through electrostatic interaction, and the adsorption equilibrium will be gradually reached as the adsorption sites of the surface layer are occupied (Chen et al., 2021). The fitting results of the adsorption kinetics of the PS group showed that the PSO model fitted better at low initial Tl(I) concentration, and the distance to the data points was closer than that of the PFO model, which indicated that chemical adsorption might be the main mechanism for adsorption between PS and Tl(I) (Ho and McKay, 2000; Santos et al., 2021). The chemical mechanism may involve electron sharing and exchanging, complexation, coordination and/or chelation between Tl(I) and MPs (Martinez-Jimenez et al., 2021). Based on the theory proposed by Weber and Morris (Weber and Boell, 1962), the Weber and Morris Model was used to identify the intra-particle diffusion mechanism (Figure S1). The fitted curve did not pass through the origin, which indicated that internal diffusion was not the main factor affecting adsorption between PS and Tl(I). According to the fitting results of the three models, it was indicated that the key mechanism of PS adsorption of Tl(I) was chemical bonding. We used ATR-FTIR and XPS to further elucidate the adsorption mechanisms.

Adsorption isotherms

Langmuir and Freundlich models were used to fit the sorption isotherm data (Figure 2), and the full model summaries are presented in Tables S5-S8. Both Langmuir and Freundlich models fitted sorption data of "particle size group" and "pH group" of PS well. However, the Freundlich model fitted better than the Langmuir model (Table S5), which indicated that the adsorption of PS to Tl(I) was mainly nonlinear adsorption. The uneven distribution of adsorption sites can cause nonlinear adsorption, which might be explained by specific adsorbate-adsorbent interactions; nonlinear adsorption also occurred when pore filling is involved in the adsorption process (Zhang et al., 2018; Dong et al., 2020). Using both Langmuir and Freundlich models indicated this process could be roughly divided into three stages. During Stage I, a mono-molecular Tl layer was formed on PS and there was no interaction between the adsorbed Tl molecules. The adsorption rate was fast. When the surface monolayer was full, it entered the second stage (Freundlich, 1962; Tang et al., 2021b). During Stage II, with the increasing of Tl(I) concentration, Tl(I) diffused into the cracks and voids on the PS surface, and the adsorption rate

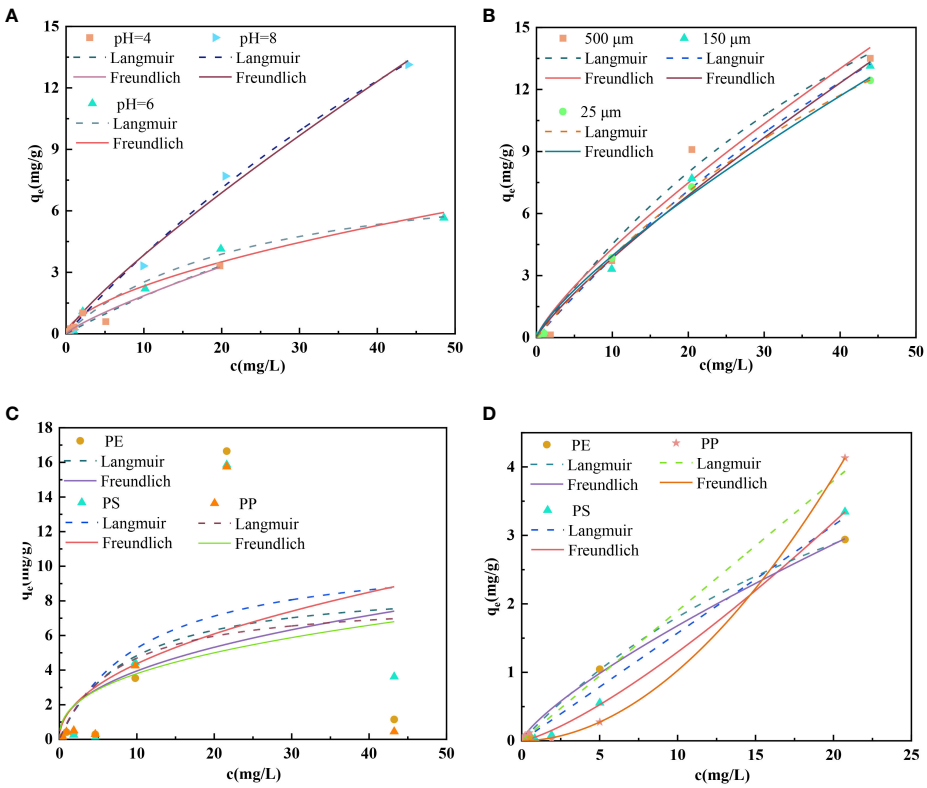

FIGURE 2
Adsorption isotherms of Tl(I) on microspheres. **(A)** PS with different pH; **(B)** PS with different particle sizes; **(C)** MPs in seawater (salinity of 32‰); **(D)** MPs in seawater (salinity of 15‰).

became slow, which formed a multilayer adsorption (Davranche et al., 2019). During Stage III, most of the adsorption sites on PS were occupied, while the concentration of Tl(I) continued to increase but could not continue to be adsorbed by PS. Therefore, the adsorption curve at this stage showed a stable trend (Hüffer et al., 2018a; Wu et al., 2019).

In the "particle size group" of PE, when the particle size was 550 μm, the Langmuir model had a higher fitting degree, which was better than the Freundlich model; when the particle size was 150 μm, the Langmuir and Freundlich models had similar fitting degrees and were both weaker than 550 μm; At 25 μm, both models fit poorly (Shown in Table S4). It showed that when the particle size of PE was large, the adsorption of Tl(I) may be mainly linear adsorption, and the adsorbed Tl^+ was distributed in a monolayer on the surface of PE. The smaller the particle size is, the worse the fitting degree of the two models is. It may be that the smaller the particle size of PE, the easier it was to float on the surface of the solution, resulting in unstable adsorption. In the "pH group" of PE, when pH=4, the fitting degree of Langmuir and Freundlich models were both higher. When pH=6, the fitting degree of Freundlich model was higher than that of Langmuir model. When pH=8, the fitting degree of the two models was similar. (Table S4). Under the conditions of pH=6 and pH=8, by comparing ATR-FTIR and XPS results of the pristine MPs and the MPs after adsorption experiment, it was found that the characteristic peaks of the three MPs fractions vibrated or elongated, the O/C ratio increased. This phenomenon was more obvious especially when pH=6. Usually, the vibration or elongation of characteristic peaks indicate surface changes of MPs (such as the appearance of wrinkles or cracks), thus aging and cracking may have occurred at lower pH conditions (Mo et al., 2021; Xu et al., 2021; Song et al., 2022). Under acidic conditions, the adsorption of Tl(I) by PE was mainly nonlinear adsorption, which means that at low pH, the concentration of H^+ was higher, which accelerated the aging and rupture of PE (Koutnik et al., 2021). After Tl^+ was adsorbed on the surface of PE, it began to be absorbed on the active sites inside the cracks. When the pH reached weak alkaline, the aging degree was weakened, and the adsorption was mainly linear adsorption.

In the "particle size group" of PP, the Langmuir model fitted better when the particle size was 13 μm, while the fitting effect of both models was poor when the particle size was 150 μm and 550 μm (Shown in Table S7). The reason may be that the smaller the particle size of PP, the larger the specific surface area, thus the adsorption performance better. In the "pH group" of PP, both models fitted well at pH=4 and pH=6, while both models fitted poorly at pH=8 (Table S7). It showed that the high concentration of H^+ in the solution promoted the adsorption of PP to Tl(I).

In the "seawater group", when the seawater salinity was 15‰, the Freundlich model fitted better for the three MPs; when the seawater salinity was 32‰, the fitting results of the two models were not good (Table S8). When the seawater salinity was 32‰, there were many kinds of ions coexisting in the system, and the concentration of the coexisting ions was much higher than that of Tl(I), resulting in poor adsorption performance for Tl(I).

In addition, some groups in the experiment did not reach the adsorption equilibrium state in the prepared concentration range of 0-50 mg/L for 7 days (Figure S2). According to the analysis of the experimental data, a higher concentration of Tl(I) solution might be required to reach the equilibrium state, whereas when the concentration was too high, it would far exceed the concentration of Tl(I) in the actual environment, which had no practical significance. Therefore, the highest concentration of Tl(I) was set to 50 mg/L. Another very important reason was that the three MPs selected in the experiment may not form tight complexes with Tl(I) due to their own density, void structure and internal dopants, and the interaction was weak, thus MPs adsorbed Tl(I) ions were easily re-desorbed. In addition, some MPs floated above the solution during the experiment, resulting in the lack of regularity in the final adsorption data.

Morphologies and surface functional groups of MPs

Pristine PS (25 μm), PE (25 μm), and PP (13 μm) and after adsorption of Tl(I) in kinetic experiments were characterized by SEM (Figure 3). Pristine PE were in spherical shape and with smooth surface. Pristine PS exhibited an irregular block structure. Pristine PP were fibrous. After adsorption kinetic experiments, the surface morphology of three MPs showed slightly rough, but the changes were small. This phenomenon may be that when the magnetic stirrer stirred, the friction between MPs particles caused physical wear (Wang et al., 2020). In addition, Chen et al. studied the adsorption of heavy metals by PS, the results showed that oxygen-containing functional groups played a dominant role in the adsorption process of heavy metals (Chen et al., 2021). The O atoms on the surface of MPs can donate a pair of lone electrons for metal ion to bond with the surface. The O element participates in the complexation to vibrate the long carbon chain, thus causing wrinkles or cracks on the surface of MPs. Therefore, it is speculated that the changes of PS surface may be caused by the involvement of O element in complexation.

Figure 4 shows the comparison of the surface functional groups on the surface of MPs (0.01 M NaCl, particle size 150 μm) after adsorption of Tl(I) ions and the functional groups on the original MPs surface in the kinetic experiment. For PE, deformation vibration and bending of carbon-long chain were observed at 670 cm^{-1} and 1468 cm^{-1}, respectively; CH_2 symmetric stretch occurred at 2850 cm^{-1} and 2919 cm^{-1} (Wang et al., 2020). For PP, deformation vibration of C-H

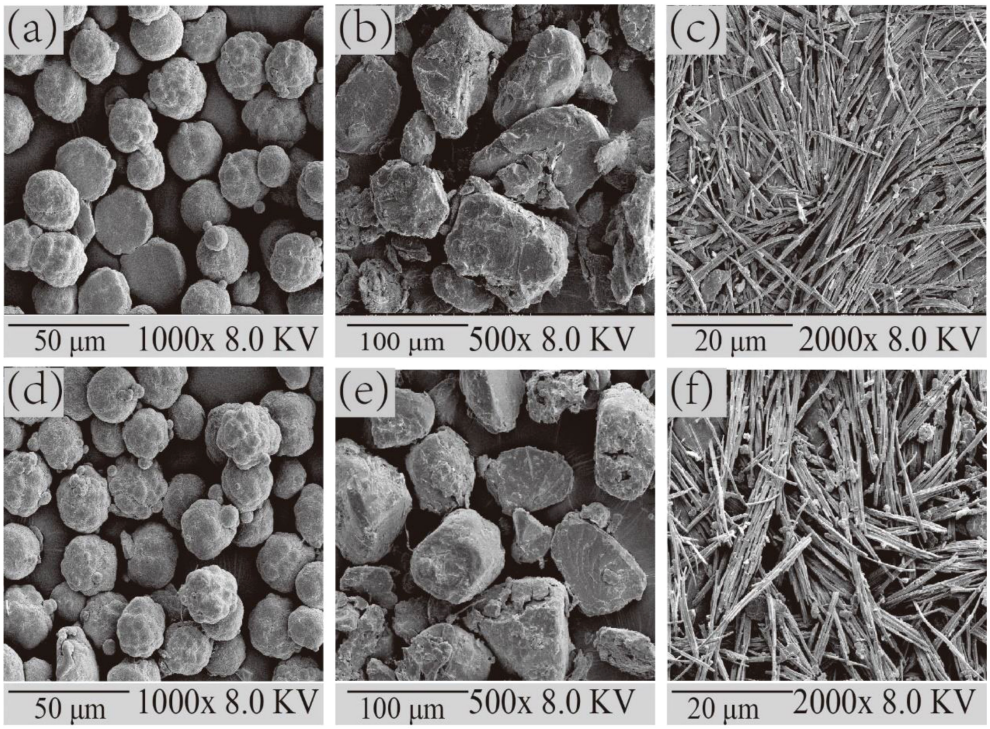

FIGURE 3
Scanning electron microscopy (SEM) images. Before adsorption **(A)** PE, **(B)** PS and **(C)** PP; after adsorption **(D)** PE, **(E)** PS and **(F)** PP.

bonds was observed at 2921 cm^{-1} and 1468-719 cm^{-1}, C-H bonds stretch occurred at 2850-2960 cm^{-1} (Imel et al., 2015). Most of the functional groups of PE and PP showed vibration or bending deformation, which might be mainly caused by the cracks generated on the surface of MPs (Matoušek et al., 2016; Wang et al., 2018) Several key absorption peaks obtained for PE and PP in this study agreed well with a previous study (Wang et al., 2018). After the adsorption of Tl(I), the composition of the functional group did not change obviously, which also indicated that the mechanism in the adsorption of Tl(I) by PE and PP might predominant be the physical adsorption governed by monolayer coverage (Yu et al., 2020).

The infrared characteristic absorption peaks for typical functional groups of pristine PS were as follows: aromatic C-H bonds at 755 cm^{-1}, C-H bonds of carbon backbone at 1026 cm^{-1}, phenyl ring at 1598 cm^{-1}, CH_2 stretching at 2920 cm^{-1}, 2850 cm^{-1} and 1450 cm^{-1}, C-H aromatic stretching at 3027 cm^{-1}, and four C=O bonds at 1742~1942 cm^{-1} (Chen et al., 2020). After the adsorption of Tl(I), the corresponding C-H bonds at 1450 cm^{-1}, 2850 cm^{-1} and 2920 cm^{-1} were significantly elongated. It indicated that the adsorption mechanism of PS to Tl(I) is complexation (Zhou et al., 2022). The involvement of O element in the complexation weakened the intermolecular interaction in PS, which led to local plasticization of the PS surface and accelerated the formation of cracks (Hüffer et al., 2018b; Dong et al., 2020; Bhagwat et al., 2021).

Surface element compositions of MPs

C and O were the main elements on the surface of MPs (> 80% of the total elements) (XPS spectral analysis results are shown in Table 1). Generally, O/C ratio has a significant effect on the adsorption performance of MPs to heavy metals. The higher the O/C ratio, the more oxygen-containing functional groups on the surface of MPs, and the better the adsorption performance (Chen et al., 2021). In pristine PE (550 μm), PS (550μm) and PP (550 μm), the O/C ratio were 0.03, 0.164 and 0.015, respectively. The O/C ratio of pristine PS was higher than that of PE and PP, indicating that pristine PS had higher contents of surface oxygen-containing functional groups. PS also exhibited a higher adsorption capacity in the "particle size group" and "pH group" in the adsorption isotherm experiments (Figure S3). After the adsorption, the O/C ratios of the three MPs with the particle size of 25 μm all increased to varying degrees (Table 1), among which the O/C ratio in PE increased the most, indicating that PE had the greatest degree of aging

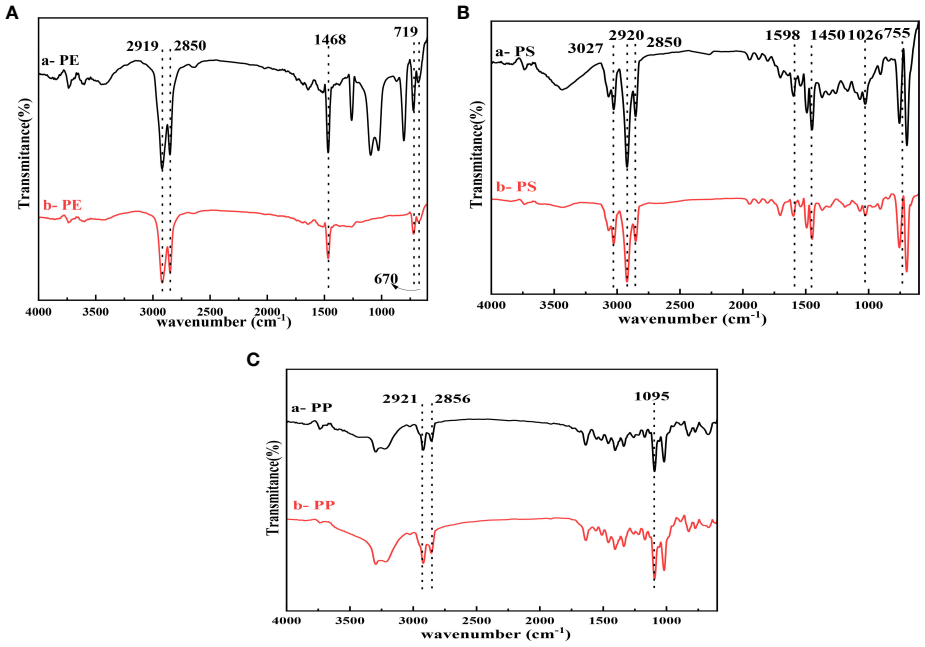

FIGURE 4
FTIR spectra of adsorption kinetics of Tl(I) on microspheres (0.01 M NaCl, 150 μm). **(A)** PE (150 μm), **(B)** PS (150 μm), **(C)** PP (150 μm). ("a" means after adsorption, "b" means before adsorption).

(Matoušek et al., 2016; Wang et al., 2018; Chen et al., 2021). Among the three MPs with the particle size of 550 μm, the O/C ratio in PE increased, and the O/C ratio in PP was almost unchanged. In addition, the O/C ratio of PS was much lower, which might be because O element participated in the complexation, resulting in the reduction of the O/C ratio. In natural seawater (pH=~8.1) and terrestrial freshwater (pH=~6-7), the zeta potential of PS is usually negative, also indicating that PS has a strong adsorption potential for Tl(I) (Tang et al., 2021a).

There were also Si and F elements on the surface of the MPs (Figure S4), which might be due to the addition of plasticizers, additives and fillers in the plastic production process (Chen et al., 2021). Cations such as Si may compete with Tl(I) element for adsorption sites on the surface of MPs, thus affecting the adsorption of Tl(I) by MPs (Tang et al., 2021b).

TABLE 1 Atomic percentages (%) for the elements on the particle surfaces before and after Tl adsorption in the kinetic adsorption [a].

Particle	type	Size (μm)	Tl concentration (mg/L)	C 1s	O 1s	F 1s	Si 2p	O/C
PE	Pristine	550	0	49.3	1.5	0	0	0.030
		25	0	42.1	0.3	0	0	0.007
	after adsorption	550	1	37.3	10.4	1.3	8.9	0.279
		25	20	21.9	7.7	0	7.3	0.352
PS	Pristine	550	0	29.3	4.81	0.4	0	0.164
		25	0	41.9	3.5	0	0	0.084
	after adsorption	550	1	44.4	0.8	7.4	0.2	0.018
		25	20	41.9	7.0	0	4.1	0.167
PP	Pristine	550	0	40.0	0.6	1.3	0	0.015
		13	0	39.8	4.1	0	0	0.103
	after adsorption	550	1	44.3	0.7	7.3	0.2	0.016
		13	20	42.4	8.2	0	0	0.193

[a]PE, polyethylene; PS, polystyrene and PP, polypropylene.

Effect of initial pH on the adsorption

Most common polymers in the environments (such as PE, PS and PP) have low pH values of isoelectric point (IEP) (Liu et al., 2022). The IEP of PP is about 4, PE is 6.5, and PS is 4.3 which means that the surfaces of MPs are negatively charged at the pH value of the natural water environment (Matoušek et al., 2016; Lin et al., 2021). The adsorption of Tl(I) by the three MPs in the "pH group" showed strong pH-dependency (Figure 2) (Dong et al., 2020; Wang et al., 2020; Zou et al., 2020). The adsorption capacity of MPs to Tl(I) at pH=4 was lower than at pH=6 (Figure S3). At the same pH, the adsorption capacity of PS to Tl(I) was higher than that of PE and PP (Figure S3A). The adsorption capacity of MPs to Tl(I) at pH=4 was lower than at pH=6 (Figure S3). The main reason for this phenomenon is that when the pH of the solution is low, H^+ competes with Tl(I) for effective adsorption sites on MPs (Liu et al., 2012), thereby reducing the adsorption of Tl(I) by MPs (Wang et al., 2021; Wang et al., 2021). When the pH of the solution was low, H^+ competed with Tl(I) for the effective adsorption sites on MPs (Liu et al., 2012), thus reducing the adsorption capacity of MPs to Tl(I) (Wang et al., 2021). At pH=8, the surface functional groups of PE (550 μm) and PP (550 μm) did not significantly change (Figure S5). However, the surface functional groups of PS (550 μm) changed, that is, hydroxyl groups were generated at 3356 cm^{-1}, and carbonyl groups were generated at 1642 cm^{-1} (Figure S5C). With the increase of pH, the deprotonation of the carboxyl functional groups on the PS surface was enhanced, and new active functional groups were formed, which increased the effective adsorption sites on the PS surface and promoted the adsorption of Tl(I) (Tang et al., 2021b).

Influence of water salinity on the adsorption

Studies have shown that the increase of salinity reduce the adsorption of metal ions by MPs, such as the competitive adsorption between Na and trace metals (e.g., Pb, Cd, Zn and Cu) (Q. Turner et al., 2020; Zhou et al., 2020; Fu et al., 2021; Qi et al., 2021; Tang et al., 2021b). In the seawater (salinity 32‰), the main cations included K^+ (37.4 mg/L), Na^+ (760.0 mg/L), Ca^{2+} (43.8 mg/L), Mg^{2+} (98.3 mg/L) and Sr^{2+} (0.75 mg/L). The total concentration of cations in seawater (salinity 32‰) was not only higher than that of seawater (salinity 15‰), but was also much higher than the highest concentration of Tl (50mg/L) in all the adsorption groups (In the seawater (salinity 15‰), the main cations included K^+ (19.4 mg/L), Na^+ (396.6 mg/L), Ca^{2+} (22.7 mg/L), Mg^{2+} (50.3 mg/L) and Sr^{2+} (0.34 mg/L)). Compared within seawater (salinity 15‰), the adsorption capacity of the three MPs on Tl(I) was lower in seawater (salinity 15‰) (Figure S2). The adsorption sites of MPs to Tl(I) include inner coordination sites and outer obligate adsorption sites. When the concentration of coexisting cations is high, they will not only form competitive adsorption with Tl(I), but may also undergo complexation reactions on the surface of MPs, resulting in a decrease in the number of inner coordination sites and outer obligate adsorption sites (Dong et al., 2020). Moreover, the large amount of Cl^- ions in seawater may promote the formation of Tl-Cl^- complexes, leading to a decrease in the activity of Tl(I) (Wang et al., 2019). In seawater systems with different salinity, the thickness of the double electron layer is different, which may affect the adsorption of Tl(I) on the surface and the diffusion inside MPs (Singh et al., 2019). In addition, compressing the double electron layer also promotes the aggregation of MPs, and further affects the adsorption capacity of MPs for Tl(I) (Wu et al., 2019; Binda et al., 2021).

Influence of self-characters of MPs on the adsorption

The common MPs in water environments include PE, PS, PP, polyethylene terephthalate (PET), polyvinyl chloride (PVC) and polylactic acid (PA). Different types of MPs have different adsorption affinities for heavy metals, which are often related to the specific surface area, polarity, crystallinity, and functional groups of MPs (Song et al., 2022). In this study, the specific surface area of MPs with the same particle size was PS > PP > PE, while the crystallinity was PE > PP > PS. MPs content crystalline regions and amorphous regions. Crystalline regions affects the adsorption of heavy metals by MPs (Fu et al., 2021). The increase in the crystallinity of MPs will lead to a decrease in the adsorption capacity and adsorption rate of heavy metals (Sun et al., 2022). Since the crystallinity is PE > PP > PS, the adsorption capacity of PS is the largest. Although particle size had a certain effect on the quasi-equilibrium time of Tl(I) adsorption on MPs, the effect of surface functional groups was more significant (Figure 4). Surface functional groups of pristine PE, PS and PP were mainly C-H, H-C-H, C-O bonds (> 80%) (Tables S9-S14), whereas the highly reactive functional groups were relatively minimal. In addition, the O/C ratios of the original MPs were low (Table 1), ranging from 0.01 to 0.36, which were much lower than that of natural minerals (the lowest O/C ratio is 0.45) (Chen et al., 2021). Therefore, MPs show poor adsorption capacity for metals compared to natural minerals (Chen et al., 2022).

The density of MPs also affects their distribution in water, which indirectly affects the adsorption of Tl by MPs. In our study, the density of PS was greater than that of water, while the densities of PE and PP were lower than that of water, thus PE and PP were more inclined to float on the water surface and had relatively less contact with Tl(I) (Wu et al., 2019), making the final adsorption lower than that of PS (Figure S3).

Influence of self-characters of Tl on the adsorption

In the current research on the adsorption of heavy metals by MPs, the metals mainly involved are chromium (Cr), cadmium (Cd), copper (Cu), lead (Pb), arsenic (As), nickel (Ni), cobalt (Co) and manganese (Mn) (Davranche et al., 2019; Li et al., 2021; Santos et al., 2021; Tang et al., 2021b; Torres et al., 2021; Fred-Ahmadu et al., 2022; Liu et al., 2022; Ren et al., 2022). Most of these metals are transition elements of the fourth period, which have unfilled *d* orbitals, and have only 1 or 2 electrons in the outermost shell, thus exhibiting abundant valence electron configurations (Lu et al., 2012). Pb (II) is more active than Cu (II); the former has higher ion exchange capacity and partition coefficient, and is easier to form an outer spherical complex with the adsorption center on the surface of MPs (Jiang et al., 2022; Liu et al., 2022). The adsorption mechanism between Cd (II) and MPs is mainly the interaction between oxygen-containing functional groups (C-O and C=O) and cation-π interaction (Aghilinasrollahabadi et al., 2021). In this study, the main adsorption mechanism of Tl(I) by PS was the polar interaction of benzene ring structure and the interaction of cation-π bond, while the adsorption of Tl(I) by PE and PP were mainly through van der Waals force which is relatively weak (Holmes et al., 2014; Zhou et al., 2020; Gao et al., 2021). Tl has lithophilic and thiophilic properties, but shows weak interactions with most organic pollutants, and seldom forms strong complexes. In most cases, Tl(I) is only loosely bound to organic polymers such as humic and fulvic acids at exchange sites (Liu et al., 2011). Besides, due to the electronic configuration characteristics of Tl ($[Xe]4f^{14}5d^{10}6s^2$), there are two bonding electrons in the 6*s* orbital of Tl(I), which can resist the formation of covalent bonds (Jacobson et al., 2005; Song et al., 2022), so Tl(I) usually only participates in exchange adsorption.

Conclusions

In this study, pristine PE were in spherical shape and with a smooth surface, pristine PS exhibited an irregular block structure and pristine PP were fibrous. After the adsorption experiment, they all showed different degrees of aging. PS showed the lowest crystallinity and had most oxygen-containing functional groups among the studied MPs, thus PS had the highest adsorption capacity for Tl(I), whereas the main adsorption mechanism of Tl(I) on PE and PP was physical adsorption. At the low initial Tl(I) concentration, crystallinity and particle size were important factors affecting adsorption of the three MPs. The aggregation phenomenon of PE was more visible at high initial Tl(I) concentrations. With the increase of pH, the deprotonation of the carboxyl functional groups on the PS surface was enhanced, which promoted the adsorption of Tl(I). The increase of salinity reduced the adsorption of Tl(I) by MPs because the coexisting cations undergo complexation reactions on the surface of MPs, leading to a decrease in the number of adsorption sites.

Generally, this study found that the adsorptions between Tl (I) and the three major MPs (PE, PP, PS) in fresh and sea water were weak, so it seems difficult for Tl(I) and MPs to form strong complexes. Therefore, these types of MPs are less likely to affect the transport of Tl in the actual environment or to produce combined toxic effects on organisms with Tl. However, studies on the potential transport mechanism of Tl by MPs in natural environments are still extremely limited. We suggest to carry out more field experiments in the future research, focusing on the species, content, surface morphology, functional groups of MPs in the real nature environments, and also consider the competitive adsorption of Tl between MPs and natural minerals (such as manganese oxide, iron oxide and clay minerals).

Data availability statement

The original contributions presented in the study are included in the article/Supplementary Material. Further inquiries can be directed to the corresponding author.

Author contributions

ML: Investigation, Resources, Data curation, Writing - review & editing. XS: Investigation, Resources, Writing - review & editing. QW: Data curation, Writing - review & editing. SL: Data curation, Writing - review & editing. SK: Data curation, Writing - review & editing. ZG: Supervision, Resources, Funding acquisition. WZ: Conceptualization, Methodology, Investigation, Supervision, Resources, Data curation, Funding acquisition, Writing - review & editing. All authors contributed to the article and approved the submitted version.

Funding

The authors acknowledge financial support from the Natural Science Foundation of Shandong Province, China (NO. ZR2020MD074) and Wenhai Program of the S&T Fund of Shandong Province for Pilot National Laboratory for Marine Science and Technology (Qingdao) (NO. 2021WHZZB0900).

Conflict of interest

Authors SL and SK were employed by company Hebei Zhong Xu inspection testing technologies Co, Ltd.

The remaining authors declare that the research was conducted in the absence of any commercial or financial relationships that could be construed as a potential conflict of interest.

Publisher's note

All claims expressed in this article are solely those of the authors and do not necessarily represent those of their affiliated organizations, or those of the publisher, the editors and the reviewers. Any product that may be evaluated in this article, or claim that may be made by its manufacturer, is not guaranteed or endorsed by the publisher.

Supplementary material

The Supplementary Material for this article can be found online at: https://www.frontiersin.org/articles/10.3389/fmars.2022.1033164/full#supplementary-material

References

Aghilinasrollahabadi, K., Salehi, M., and Fujiwara, T. (2021). Investigate the influence of microplastics weathering on their heavy metals uptake in stormwater. *J. Hazard. Mater.* 408, 124439. doi: 10.1016/j.jhazmat.2020.124439

Belzile, N., and Chen, Y. W. (2017). Thallium in the environment: A critical review focused on natural waters, soils, sediments and airborne particles. *Appl. Geochem.* 84, 218–243. doi: 10.1016/j.apgeochem.2017.06.013

Bhagwat, G., Tran, T. K. A., Lamb, D., Senathirajah, K., Grainge, I., O'Connor, W., et al. (2021). Biofilms enhance the adsorption of toxic contaminants on plastic microfibers under environmentally relevant conditions. *Environ. Sci. Technol.* 55, 8877–8887. doi: 10.1021/acs.est.1c02012

Binda, G., Spanu, D., Monticelli, D., Pozzi, A., Bellasi, A., Bettinetti, R., et al. (2021). Unfolding the interaction between microplastics and (trace) elements in water: A critical review. *Water Res.* 204, 117637. doi: 10.1016/j.watres.2021.117637

Borgmann, U., Cheam, V., Norwood, W. P., and Lechner, J. (1998). Toxicity and bioaccumulation of thallium in hyalella azteca, with comparison to other metals and prediction of environmental impact. *Environ. pollut.* 99, 105–114. doi: 10.1016/S0269-7491(97)00181-4

Cao, Y., Zhao, M., Ma, X., Song, Y., Zuo, S., Li, H., et al. (2021). A critical review on the interactions of microplastics with heavy metals: Mechanism and their combined effect on organisms and humans. *Sci. Total Environ.* 788, 147620. doi: 10.1016/j.scitotenv.2021.147620

Chen, G., Fu, Z., Yang, H., and Wang, J. (2020). An overview of analytical methods for detecting microplastics in the atmosphere. *TrAC - Trends Anal. Chem.* 130, 115981. doi: 10.1016/j.trac.2020.115981

Chen, W., Xiong, J., Liu, J., Wang, H., Yao, J., Liu, H., et al. (2022). Thermodynamic and kinetic coupling modeling for thallium(I) sorption at a heterogeneous titanium dioxide interface. *J. Hazard. Mater.* 428, 128230. doi: 10.1016/j.jhazmat.2022.128230

Chen, C. C., Zhu, X., Xu, H., Chen, F., Ma, J., and Pan, K. (2021). Copper adsorption to microplastics and natural particles in seawater: A comparison of kinetics, isotherms, and bioavailability. *Environ. Sci. Technol.* 55, 13923–13931. doi: 10.1021/acs.est.1c04278

Cruz-Hernández, Y., Villalobos, M., Marcus, M. A., Pi-Puig, T., Zanella, R., and Martínez-Villegas, N. (2019). Tl(I) sorption behavior on birnessite and its implications for mineral structural changes. *Geochim. Cosmochim. Acta* 248, 356–369. doi: 10.1016/j.gca.2019.01.020

Davranche, M., Veclin, C., Pierson-Wickmann, A. C., El Hadri, H., Grassl, B., Rowenczyk, L., et al. (2019). Are nanoplastics able to bind significant amount of metals? *lead example Environ. pollut.* 249, 940–948. doi: 10.1016/j.envpol.2019.03.087

Dong, Y., Gao, M., Song, Z., and Qiu, W. (2020). As(III) adsorption onto different-sized polystyrene microplastic particles and its mechanism. *Chemosphere* 239, 124792. doi: 10.1016/j.chemosphere.2019.124792

D'Orazio, M., Campanella, B., Bramanti, E., Ghezzi, L., Onor, M., Vianello, G., et al. (2020). Thallium pollution in water, soils and plants from a past-mining site of Tuscany: Sources, transfer processes and toxicity. *J. Geochem. Explor.* 209, 106434. doi: 10.1016/j.gexplo.2019.106434

Fred-Ahmadu, O. H., Ayejuyo, O. O., Tenebe, I. T., and Benson, N. U. (2022). Occurrence and distribution of micro(meso)plastic-sorbed heavy metals and metalloids in sediments, gulf of Guinea coast (SE Atlantic). *Sci. Total Environ.* 813, 152650. doi: 10.1016/j.scitotenv.2021.152650

Freundlich, J. (1962). Kennzeichnung von elektroden und elktrodenmaterialien MIT HILFE DER UND DER INNEREN OBERFLÄCHE. *Electrochim. Acta* 8, 35–50. doi: 10.1016/0013-4686(62)87022-4

Fu, L., Li, J., Wang, G., Luan, Y., and Dai, W. (2021). Adsorption behavior of organic pollutants on microplastics. *Ecotoxicol. Environ. Saf.* 217, 112207. doi: 10.1016/j.ecoenv.2021.112207

Fu, Q., Tan, X., Ye, S., Ma, L., Gu, Y., Zhang, P., et al. (2021). Mechanism analysis of heavy metal lead captured by natural-aged microplastics. *Chemosphere* 270, 128624. doi: 10.1016/j.chemosphere.2020.128624

Gao, X., Hassan, I., Peng, Y., Huo, S., and Ling, L. (2021). Behaviors and influencing factors of the heavy metals adsorption onto microplastics: A review. *J. Clean Prod.* 319, 128777. doi: 10.1016/j.jclepro.2021.128777

Ghezzi, L., D'Orazio, M., Doveri, M., Lelli, M., Petrini, R., and Giannecchini, R. (2019). Groundwater and potentially toxic elements in a dismissed mining area: Thallium contamination of drinking spring water in the apuan Alps (Tuscany, Italy). *J. Geochem. Explor.* 197, 84–92. doi: 10.1016/j.gexplo.2018.11.009

Holmes, L. A., Turner, A., and Thompson, R. C. (2014). Interactions between trace metals and plastic production pellets under estuarine conditions. *Mar. Chem.* 167, 25–32. doi: 10.1016/j.marchem.2014.06.001

Ho, Y. S., and McKay, G. (2000). The kinetics of sorption of divalent metal ions onto sphagnum moss peat. *Water Res.* 34, 735–742. doi: 10.1016/S0043-1354(99)00232-8

Horn, D. A., Granek, E. F., and Steele, C. L. (2020). Effects of environmentally relevant concentrations of microplastic fibers on pacific mole crab (Emerita analoga) mortality and reproduction. *Limnol. Oceanogr. Lett.* 5, 74–83. doi: 10.1002/lol2.10137

Huang, D., Tao, J., Cheng, M., Deng, R., Chen, S., Yin, L., et al. (2021). Microplastics and nanoplastics in the environment: Macroscopic transport and effects on creatures. *J. Hazard. Mater.* 407, 124399. doi: 10.1016/j.jhazmat.2020.124399

Hüffer, T., Weniger, A. K., and Hofmann, T. (2018a). Sorption of organic compounds by aged polystyrene microplastic particles. *Environ. pollut.* 236, 218–225. doi: 10.1016/j.envpol.2018.01.022

Hüffer, T., Weniger, A. K., and Hofmann, T. (2018b). Data on sorption of organic compounds by aged polystyrene microplastic particles. *Data Br.* 18, 474–479. doi: 10.1016/j.dib.2018.03.053

Imel, A., Malmgren, T., Dadmun, M., Gido, S., and Mays, J. (2015). *In vivo* oxidative degradation of polypropylene pelvic mesh. *Biomaterials* 73, 131–141. doi: 10.1016/j.biomaterials.2015.09.015

Jacobson, A. R., McBride, M. B., Baveye, P., and Steenhuis, T. S. (2005). Environmental factors determining the trace-level sorption of silver and thallium to soils. *Sci. Total Environ.* 345, 191–205. doi: 10.1016/j.scitotenv.2004.10.027

Jiang, Y., Qin, Z., Fei, J., Ding, D., Sun, H., Wang, J., et al. (2022). Surfactant-induced adsorption of Pb(II) on the cracked structure of microplastics. *J. Colloid Interface Sci.* 621, 91–100. doi: 10.1016/j.jcis.2022.04.068

Kim, T.-K. K., Jang, M., and Hwang, Y. S. (2022). Adsorption of benzalkonium chlorides onto polyethylene microplastics: Mechanism and toxicity evaluation. *J. Hazard. Mater.* 426, 128076. doi: 10.1016/j.jhazmat.2021.128076

Kiseeva, E. S., and Wood, B. J. (2013). A simple model for chalcophile element partitioning between sulphide and silicate liquids with geochemical applications. *Earth Planet. Sci. Lett.* 383, 68–81. doi: 10.1016/j.epsl.2013.09.034

Koutnik, V. S., Leonard, J., Alkidim, S., DePrima, F. J., Ravi, S., Hoek, E. M. V., et al. (2021). Distribution of microplastics in soil and freshwater environments: Global analysis and framework for transport modeling. *Environ. Pollut.* 274, 116552. doi: 10.1016/j.envpol.2021.116552

Kutralam-Muniasamy, G., Pérez-Guevara, F., Martínez, I. E., and Shruti, V. C. (2021). Overview of microplastics pollution with heavy metals: Analytical methods, occurrence, transfer risks and call for standardization. *J. Hazard. Mater.* 415, 125755. doi: 10.1016/j.jhazmat.2021.125755

Lan, C. H., and Lin, T. S. (2005). Acute toxicity of trivalent thallium compounds to daphnia magna. *Ecotoxicol. Environ. Saf.* 61, 432–435. doi: 10.1016/j.ecoenv.2004.12.021

Li, J., Huang, X., Hou, Z., and Ding, T. (2022). Sorption of diclofenac by polystyrene microplastics: Kinetics, isotherms and particle size effects. *Chemosphere* 290, 133311. doi: 10.1016/j.chemosphere.2021.133311

Li, Y., Li, M., Li, Z., Yang, L., and Liu, X. (2019). Effects of particle size and solution chemistry on triclosan sorption on polystyrene microplastic. *Chemosphere* 231, 308–314. doi: 10.1016/j.chemosphere.2019.05.116

Li, M., Liu, Y., Xu, G., Wang, Y., and Yu, Y. (2021). Impacts of polyethylene microplastics on bioavailability and toxicity of metals in soil. *Sci. Total Environ.* 760, 144037. doi: 10.1016/j.scitotenv.2020.144037

Lin, W. H., Kuo, J., and Lo, S. L. (2021). Effect of light irradiation on heavy metal adsorption onto microplastics. *Chemosphere* 285, 131457. doi: 10.1016/j.chemosphere.2021.131457

Lin, J., Yin, M., Wang, J., Liu, J., Tsang, D. C. W., Wang, Y., et al. (2020). Geochemical fractionation of thallium in contaminated soils near a large-scale Hg-tl mineralised area. *Chemosphere* 239, 124775. doi: 10.1016/j.chemosphere.2019.124775

Liu, S., Huang, J. H., Zhang, W., Shi, L. X., Yi, K. X., Zhang, C. Y., et al. (2022). Investigation of the adsorption behavior of Pb(II) onto natural-aged microplastics as affected by salt ions. *J. Hazard. Mater.* 431, 128643. doi: 10.1016/j.jhazmat.2022.128643

Liu, J., Lippold, H., Wang, J., Lippmann-Pipke, J., and Chen, Y. (2011). Sorption of thallium(I) onto geological materials: Influence of pH and humic matter. *Chemosphere* 82, 866–871. doi: 10.1016/j.chemosphere.2010.10.089

Liu, Z., Qin, Q., Hu, Z., Yan, L., Ieong, U. I., and Xu, Y. (2020). Adsorption of chlorophenols on polyethylene terephthalate microplastics from aqueous environments: Kinetics, mechanisms and influencing factors. *Environ. pollut.* 265, 114926. doi: 10.1016/j.envpol.2020.114926

Liu, Y. H., Shaheen, S. M., Rinklebe, J., and Hseu, Z. Y. (2021). Pedogeochemical distribution of gallium, indium and thallium, their potential availability and associated risk in highly-weathered soil profiles of Taiwan. *Environ. Res.* 197, 110994. doi: 10.1016/j.envres.2021.110994

Liu, J., Wang, J., Chen, Y., Lippold, H., Xiao, T., Li, H., et al. (2017). Geochemical transfer and preliminary health risk assessment of thallium in a riverine system in the pearl river basin, south China. *J. Geochem. Explor.* 176, 64–75. doi: 10.1016/j.gexplo.2016.01.011

Liu, J., Wang, J., Chen, Y., Xie, X., Qi, J., Lippold, H., et al. (2016). Thallium transformation and partitioning during Pb-zn smelting and environmental implications. *Environ. pollut.* 212, 77–89. doi: 10.1016/j.envpol.2016.01.046

Liu, J., Wang, J., Xiao, T., Bao, Z., Lippold, H., Luo, X., et al. (2018). Geochemical dispersal of thallium and accompanying metals in sediment profiles from a smelter-impacted area in south China. *Appl. Geochem.* 88, 239–246. doi: 10.1016/j.apgeochem.2017.05.013

Liu, H., Wang, X., Zhai, G., Zhang, J., Zhang, C., Bao, N., et al. (2012). Preparation of activated carbon from lotus stalks with the mixture of phosphoric acid and pentaerythritol impregnation and its application for Ni(II) sorption. *Chem. Eng. J.* 209, 155–162. doi: 10.1016/j.cej.2012.07.132

Liu, J., Yin, M., Luo, X., Xiao, T., Wu, Z., Li, N., et al. (2019). The mobility of thallium in sediments and source apportionment by lead isotopes. *Chemosphere* 219, 864–874. doi: 10.1016/j.chemosphere.2018.12.041

Lu, P., Liu, F., Xue, D., Yang, H., and Liu, Y. (2012). Phase selective route to Ni (OH) 2 with enhanced supercapacitance: Performance dependent hydrolysis of Ni (Ac) 2 at hydrothermal conditions. *Electrochim. Acta* 78, 1–10. doi: 10.1016/j.electacta.2012.03.183\

Martinez-Jimenez, F., de Arruda Ribeiro, M. P., Sargo, C. R., Ienczak, J. L, Morais, E. R., and da Costa, A. C. (2021). Dynamic modeling Application to evaluate the performance of spathaspora passalidarumin second-generation ethanol production: Parametric dynamics and the likelihood confidence region. *Ind. Eng. Chem. Res.* 60, 13822–13833. doi: 10.1021/acs.iecr.1c02299

Matoušek, J., Bendlová, N., Kolská, Z., Čapková, P., Pavlík, J., and Kormunda, M. (2016). Time dependence of the surface chemistry of the plasma treated polypropylene powder. *Adv. Powder Technol.* 27, 262–267. doi: 10.1016/j.apt.2015.12.010

Mo, Q., Yang, X., Wang, J., Xu, H., Li, W., Fan, Q., et al. (2021). Adsorption mechanism of two pesticides on polyethylene and polypropylene microplastics: DFT calculations and particle size effects. *Environ. pollut.* 291, 118120. doi: 10.1016/j.envpol.2021.118120

Nkwachukwu, O., Chima, C., Ikenna, A., and Albert, L. (2013). Focus on potential environmental issues on plastic world towards a sustainable plastic recycling in developing countries. *Int. J. Ind. Chem.* 4, 34. doi: 10.1186/2228-5547-4-34

Peacock, C. L., and Moon, E. M. (2012). Oxidative scavenging of thallium by birnessite: Explanation for thallium enrichment and stable isotope fractionation in marine ferromanganese precipitates. *Geochim. Cosmochim. Acta* 84, 297–313. doi: 10.1016/j.gca.2012.01.036

Peter, A. L. J., and Viraraghavan, T. (2005). Thallium: A review of public health and environmental concerns. *Environ. Int.* 31, 493–501. doi: 10.1016/j.envint.2004.09.003

Purwiyanto, A. I. S., Suteja, Y., Ningrum, P. S., Putri, W. A. E., Agustriani, F., Cordova, M. R., et al. (2020). Concentration and adsorption of Pb and Cu in microplastics: Case study in aquatic environment. *Mar. pollut. Bull.* 158, 111380. doi: 10.1016/j.marpolbul.2020.111380

Qi, K., Lu, N., Zhang, S., Wang, W., Wang, Z., and Guan, J. (2021). Uptake of Pb (II) onto microplastic-associated biofilms in freshwater: Adsorption and combined toxicity in comparison to natural solid substrates. *J. Hazard. Mater.* 411, 125115. doi: 10.1016/j.jhazmat.2021.125115

Ralph, L., and Twiss, M. R. (2002). Comparative toxicity of Thallium(I), Thallium(III), and Cadmium(II) to the unicellular alga isolated from lake Erie. *Bull. Environ. Contam. Toxicol.* 68, 0261–0268. doi: 10.1007/s00128-001-0247-z

Ren, S., Wei, X., Wang, J., Liu, J., Ouyang, Q., Jiang, Y., et al. (2022). Unexpected enrichment of thallium and its geochemical behaviors in soils impacted by historically industrial activities using lead–zinc carbonate minerals. *Sci. Total Environ.* 821, 153399. doi: 10.1016/j.scitotenv.2022.153399

Santos, D., Luzio, A., Matos, C., Bellas, J., Monteiro, S. M., and Félix, L. (2021). Microplastics alone or co-exposed with copper induce neurotoxicity and behavioral alterations on zebrafish larvae after a subchronic exposure. *Aquat. Toxicol.* 235, 105814. doi: 10.1016/j.aquatox.2021.105814

Singh, N., Tiwari, E., Khandelwal, N., and Darbha, G. K. (2019). Understanding the stability of nanoplastics in aqueous environments: Effect of ionic strength, temperature, dissolved organic matter, clay, and heavy metals. *Environ. Sci.* 6, 2968–2976. doi: 10.1039/c9en00557a

Song, X., Zhuang, W., Cui, H., Liu, M., Gao, T., Li, A., et al. (2022). Interactions of microplastics with organic, inorganic and bio-pollutants and the ecotoxicological effects on terrestrial and aquatic organisms. *Sci. Total Environ.* 838, 156068. doi: 10.1016/j.scitotenv.2022.156068

Sun, M., Yang, Y., Huang, M., Fu, S., Hao, Y., Hu, S., et al. (2022). Adsorption behaviors and mechanisms of antibiotic norfloxacin on degradable and nondegradable microplastics. *Sci. Total Environ.* 807, 151042. doi: 10.1016/j.scitotenv.2021.151042

Tang, S., Lin, L., Wang, X., Sun, X., and Yu, A. (2021a). Adsorption of fulvic acid onto polyamide 6 microplastics: Influencing factors, kinetics modeling, site energy distribution and interaction mechanisms. *Chemosphere* 272, 129638. doi: 10.1016/j.chemosphere.2021.129638

Tang, S., Lin, L., Wang, X., Yu, A., and Sun, X. (2021b). Interfacial interactions between collected nylon microplastics and three divalent metal ions (Cu(II), Ni(II), Zn(II)) in aqueous solutions. *J. Hazard. Mater.* 403, 123548. doi: 10.1016/j.jhazmat.2020.123548

Torres, F. G., Dioses-Salinas, D. C., Pizarro-Ortega, C. I., and De-la-Torre, G. E. (2021). Sorption of chemical contaminants on degradable and non-degradable microplastics: Recent progress and research trends. *Sci. Total Environ.* 757, 143875. doi: 10.1016/j.scitotenv.2020.143875

Turner, A., Holmes, L., Thompson, R. C., and Fisher, A. S. (2020). Metals and marine microplastics: Adsorption from the environment versus addition during manufacture, exemplified with lead. *Water Res.* 173, 115577. doi: 10.1016/j.watres.2020.115577

Wagner, M., Scherer, C., Alvarez-Muñoz, D., Brennholt, N., Bourrain, X., Buchinger, S., et al. (2014). Microplastics in freshwater ecosystems: what we know and what we need to know. *Environ. Sci. Eur.* 26, 1–9. doi: 10.1186/s12302-014-0012-7

Wang, Z., Chen, M., Zhang, L., Wang, K., Yu, X., Zheng, Z., et al. (2018). Sorption behaviors of phenanthrene on the microplastics identified in a mariculture farm in xiangshan bay, southeastern China. *Sci. Total Environ.* 628–629, 1617–1626. doi: 10.1016/j.scitotenv.2018.02.146

Wang, Z., Fu, D., Gao, L., Qi, H., Su, Y., and Peng, L. (2021). Aged microplastics decrease the bioavailability of coexisting heavy metals to microalga chlorella vulgaris. *Ecotoxicol. Environ. Saf.* 217, 112199. doi: 10.1016/j.ecoenv.2021.112199

Wang, L., Gao, Y., Jiang, W., Chen, J., Chen, Y., Zhang, X., et al. (2021). Microplastics with cadmium inhibit the growth of vallisneria natans (Lour.) hara rather than reduce cadmium toxicity. *Chemosphere* 266, 128979. doi: 10.1016/j.chemosphere.2020.128979

Wang, Y., Wang, X., Li, Y., Li, J., Wang, F., Xia, S., et al. (2020). Biofilm alters tetracycline and copper adsorption behaviors onto polyethylene microplastics. *Chem. Eng. J.* 392, 123808. doi: 10.1016/j.cej.2019.123808

Wang, F., Yang, W., Cheng, P., Zhang, S., Zhang, S., Jiao, W., et al. (2019). Adsorption characteristics of cadmium onto microplastics from aqueous solutions. *Chemosphere* 235, 1073–1080. doi: 10.1016/j.chemosphere.2019.06.196

Wang, Y., Yang, Y., Liu, X., Zhao, J., Liu, R., and Xing, B. (2021). Interaction of microplastics with antibiotics in aquatic environment: Distribution, adsorption, and toxicity. *Environ. Sci. Technol.* 55, 15579–15595. doi: 10.1021/acs.est.1c04509

Wang, J., Zhou, Y., Dong, X., Yin, M., Tsang, D. C. W., Sun, J., et al. (2020). Temporal sedimentary record of thallium pollution in an urban lake: An emerging thallium pollution source from copper metallurgy. *Chemosphere* 242, 125172. doi: 10.1016/j.chemosphere.2019.125172

Weber, R., and Boell, E. J. (1962). Enzyme patterns in isolated mitochondria from embryonic and larval tissues of xenopus. *Dev. Biol.* 4, 452–472. doi: 10.1016/0012-1606(62)90052-0

Wick, S., Baeyens, B., Marques Fernandes, M., and Voegelin, A. (2018). Thallium adsorption onto illite. *Environ. Sci. Technol.* 52, 571–580. doi: 10.1021/acs.est.7b04485

Wick, S., Peña, J., and Voegelin, A. (2019). Thallium sorption onto manganese oxides. *Environ. Sci. Technol.* 53, 13168–13178. doi: 10.1021/acs.est.9b04454

Willner, J., Fornalczyk, A., Jablonska-Czapla, M., Grygoyc, K., and Rachwal, M. (2021). Studies on the content of selected technology critical elements (Germanium, tellurium and thallium) in electronic waste. *Mater. (Basel)* 14, 3722. doi: 10.3390/ma14133722

Wu, P., Cai, Z., Jin, H., and Tang, Y. (2019). Adsorption mechanisms of five bisphenol analogues on PVC microplastics. *Sci. Total Environ.* 650, 671–678. doi: 10.1016/j.scitotenv.2018.09.049

Wu, J., Jiang, R., Lin, W., and Ouyang, G. (2019). Effect of salinity and humic acid on the aggregation and toxicity of polystyrene nanoplastics with different functional groups and charges. *Environ. pollut.* 245, 836–843. doi: 10.1016/j.envpol.2018.11.055

Xi, B., Wang, B., Chen, M., Lee, X., Zhang, X., Wang, S., et al. (2022). Environmental behaviors and degradation methods of microplastics in different environmental media. *Chemosphere* 299, 134354. doi: 10.1016/j.chemosphere.2022.134354

Xi, X., Wang, L., Zhou, T., Yin, J., Sun, H., Yin, X., et al. (2022). Effects of physicochemical factors on the transport of aged polystyrene nanoparticles in saturated porous media. *Chemosphere* 289, 133239. doi: 10.1016/j.chemosphere.2021.133239

Xu, G., Liu, Y., and Yu, Y. (2021). Effects of polystyrene microplastics on uptake and toxicity of phenanthrene in soybean. *Sci. Total Environ.* 783, 147016. doi: 10.1016/j.scitotenv.2021.147016

Yang, S.-S., Ding, M.-Q., Ren, X.-R., Zhang, Z.-R., Li, M.-X., Zhang, L.-L., et al. (2022). Impacts of physical-chemical property of polyethylene (PE) on depolymerization and biodegradation in insects yellow mealworms (Tenebrio molitor) and dark mealworms (Tenebrio obscurus) with high purity microplastics. *Sci. Total Environ.*, 828:154458. doi: 10.1016/j.scitotenv.2022.154458

Yan, X., Zhu, M., Li, W., Peacock, C. L., Ma, J., Wen, H., et al. (2021). Cadmium isotope fractionation during adsorption and substitution with iron (Oxyhydr) oxides. *Environ. Sci. Technol.* 55, 11601–11611. doi: 10.1021/acs.est.0c06927

Yao, J., Wang, H., Ma, C., Cao, Y., Chen, W., Gu, L., et al. (2022). Cotransport of thallium(I) with polystyrene plastic particles in water-saturated porous media. *J. Hazard. Mater.* 422, 126910. doi: 10.1016/j.jhazmat.2021.126910

Yu, Y., Ma, R., Qu, H., Zuo, Y., Yu, Z., Hu, G., et al. (2020). Enhanced adsorption of tetrabromobisphenol a (TBBPA) on cosmetic-derived plastic microbeads and combined effects on zebrafish. *Chemosphere* 248, 126067. doi: 10.1016/j.chemosphere.2020.126067

Yu, A., Sun, X., Tang, S., Zhang, Y., Li, M., and Wang, X. (2021). Adsorption mechanism of cadmium on polystyrene microplastics containing hexabromocyclododecane. *Environ. Technol. Innov.* 24, 102036. doi: 10.1016/j.eti.2021.102036

Zhang, Y., Jiang, H., Bian, K., Wang, H., and Wang, C. (2021). A critical review of control and removal strategies for microplastics from aquatic environments. *J. Environ. Chem. Eng.* 9, 105463. doi: 10.1016/j.jece.2021.105463

Zhang, H., Wang, J., Zhou, B., Zhou, Y., Dai, Z., Zhou, Q., et al. (2018). Enhanced adsorption of oxytetracycline to weathered microplastic polystyrene: Kinetics, isotherms and influencing factors. *Environ. pollut.* 243, 1550–1557. doi: 10.1016/j.envpol.2018.09.122

Zhou, Z., Sun, Y., Wang, Y., Yu, F., and Ma, J. (2022). Adsorption behavior of Cu (II) and Cr(VI) on aged microplastics in antibiotics-heavy metals coexisting system. *Chemosphere* 291, 132794. doi: 10.1016/j.chemosphere.2021.132794

Zhou, Y., Yang, Y., Liu, G., He, G., and Liu, W. (2020). Adsorption mechanism of cadmium on microplastics and their desorption behavior in sediment and gut environments: The roles of water pH, lead ions, natural organic matter and phenanthrene. *Water Res.* 184, 116209. doi: 10.1016/j.watres.2020.116209

Zhuang, W., Liu, M., Song, J., and Ying, S. C. (2021). Retention of thallium by natural minerals: A review. *Sci. Total Environ.* 777, 146074. doi: 10.1016/j.scitotenv.2021.146074

Zou, J., Liu, X., Zhang, D., and Yuan, X. (2020). Adsorption of three bivalent metals by four chemical distinct microplastics. *Chemosphere* 248, 126064. doi: 10.1016/j.chemosphere.2020.126064